Regular Article

Abdulrahman I. Alateyah, Mohammed Nejlaoui, Mohammed Albadrani, Abdulrahman Alrumayh, Hassan Abd El-Hafez, Hisham A. Alrumayh, Sufyan A. Alomari, Abdulaziz H. Alomayrini, Hamad H. Albazie and Waleed H. El-Garaihy*

Design optimization of a 4-bar exoskeleton with natural trajectories using unique gait-based synthesis approach

Abstract: Strolling is a complex activity that requires the synchronization of the brain, anxiety, and muscles, as well as rhythmic movement of the lower limbs. Gait may be abnormal if coordination is disrupted. As a result, exoskeletons should be used to treat it effectively. The connection and other systems contained in the exoskeletons could be used to mimic the behavior of the human lower leg. These mechanisms are created utilizing complex traditional methods. This study proposes a new gait-inspired method based on a genetic algorithm (GA) for synthesizing a four-bar mechanism for exoskeletons. For each phase of the gait, the trajectory is calculated and merged using optimization algorithms. Each phase of the trajectory passes through 10 precision points, for an entirety of 20 precision points in 1 gait cycle. For the problem under consideration, it is discovered that the GA outperforms other literature techniques. Finally, the proposed design for a lower limb exoskeleton is depicted as a solid model. Furthermore, the generated link-age accurately tracks all the transition points, and the simulation of the planned linkage for one gait cycle has been illustrated using a stick diagram.

Keywords: exoskeleton, four-bar, optimization, GA, knee, lower limb, gait-based synthesis

1 Introduction

The knee joint is an important anatomical component of the human body since it carries the body's weight throughout most of the daily activities and is prone to serious injuries and illnesses [1]. There are more and more persons with lower limb disability as a result of these illnesses and injuries (such as heart disease, stroke, trauma, and inflammation). Patients who suffer from these illnesses or traumas eventually have no or substantially diminished muscle function, which makes life more challenging for them. Some of the most prevalent issues that persons with disabilities faced are: unable to sit, stand, or move without support, depending on walkers, crutches, or wheelchairs. Commercially available assistive and rehabilitative devices exist; however, they are ineffectual and expensive [2,3].

For many of these illnesses, the medical world has yet to discover a therapy or cure. Assistive devices are one possibility for relieving symptoms while medical re-search continues. To this purpose, a lot of research has gone into developing assistive devices that can help people regain their lost range of mobility or limb functioning. Exoskeleton devices, for example, are now being employed, mostly in physical therapy, to help patients retrain paralyzed or hindered human body mobility [4].

The rehabilitation process and therapeutic procedures have been proven in research studies to improve the functionality of the rehabilitated part [4–9]. However, there are differing viewpoints on the rehabilitation principles and techniques. Early mobilization is advised by

* **Corresponding author: Waleed H. El-Garaihy,** Department of Mechanical Engineering, College of Engineering, Qassim University, Unaizah 56452, Saudi Arabia; Mechanical Engineering Department, Faculty of Engineering, Suez Canal University, Ismailia 41522, Egypt, e-mail: w.nasr@qu.edu.sat, tel: +966-551108490
Abdulrahman I. Alateyah, Mohammed Nejlaoui, Mohammed Albadrani, Abdulrahman Alrumayh, Hisham A. Alrumayh, Sufyan A. Alomari, Abdulaziz H. Alomayrini, Hamad H. Albazie: Department of Mechanical Engineering, College of Engineering, Qassim University, Unaizah 56452, Saudi Arabia
Hassan Abd El-Hafez: Department of Mechanical Engineering, College of Engineering, Qassim University, Unaizah 56452, Saudi Arabia; Production Engineering and Mechanical Design Department, Faculty of Engineering, Port-Said University, Port-Said 42523, Egypt

some physicists for greater recovery, whereas passive movements are only recommended in the early stages by others [10]. According to certain research, for a rapid recovery, specific task-based exercises for injured muscles and ligaments are preferred. The choice of rehabilitative methods is particularly important, since the wrong type of rehabilitation might result in aberrant wear, patellofemoral issues, and premature muscle relaxation [11]. The researchers demonstrate that the way a person's knee joint moves are fundamentally multi-axial, based on ergonomic principles and the human body's biomechanical design.

The human knee joint is made up of the femur, tibia, anterior cruciate ligament, posterior cruciate ligament, and knee joint [13]. When bent, the femur has a tendency to roll and slide on the tibia with a variable instantaneous center of rotation (ICR). As a result, understanding and quantifying the way the human knee joint moves is critical when constructing an exoskeleton knee joint structure. Because the knee joint in a person does not have a single axis, it is necessary to quantify the human knee joint's instantaneous rotation center and transform it into a mathematical model [12]. This mathematical model may then be examined using artificial intelligence algorithms written in MATLAB to align the locations of the exoskeleton ICR and the human knee joint ICR as close as possible.

Material selection is one of the most important phases, to ensure the capability of withstanding the impact of human load through the walking phases. The frame of the exoskeleton should be light and strong. Also, the suitable manufacturing process that can build a complicated shape and orientation. In addition, the manufacturing process should be affordable and easy to use. In this manner, the additive manufacturing is capable of building complex shapes and orientation [14]. Additive manufacturing includes 3D printing which is specified in layers building [15].

The historical exoskeletons' research and development revealed various limits in the fields of robotic control, stability, actuation, and energy supply [16]. Over the last few decades, research in these areas have been stimulated by the application to exoskeleton and other sectors [17]. Recent breakthroughs in these fields have resulted in the creation of active exoskeletons that are more capable and autonomous. Kim et al. [18] designed a powered exoskeleton based on four-bar linkage. The exoskeleton can be considered as a system that contains resistors, sensors, and encoder in the motor and this system is developed to support the knee joint of people with hemiplegia. The advantages of this powered exoskeleton are that it is used for hemiplegic patients and it weighs only 3.5 kg

[19]. The disadvantage of this powered exoskeleton is that it cannot be used for climbing up and down. Lu et al. [20] designed an exoskeleton powered by hydraulic drive for the hemiplegic patients. With the aid of Simulink, the knee joint's design was based on a four-bar link. The data used to design the four-bar are collected by experiments. Niu et al. [21] develop a powered exoskeleton design based on five-bar linkage. By adopting a five-bar connection rather than a four-bar linkage, the misalignment between the instantaneous centers of rotation of human joints and the exoskeleton is reduced. Kittisares et al. [22] proposed a four-bar linkage-based powered exoskeleton with hydraulic artificial muscle assistance to support the users who have a problem in their muscles. The verification of this study is done based experiment. The ad-vantage of this exoskeleton is the output pressure is adjustable depending on the situation of the patients. The disadvantage of this exoskeleton is designed without the power supply. A bionic knee exoskeleton based on a cross four-bar connection system is suggested by Gao et al. [23]. To achieve the instantaneous rotation center movement of the knee joint, the cross four-bar linkage mechanism is used to replicate the internal cruciate ligament of the human knee joint. A tie rod and the patella, an auxiliary limit locking component of the knee joint, are used to represent the lower limb thigh muscle. A motor drive creates the ICR motion of the knee joint. Putranto et al. [24] developed a crossed four-bar powered exoskeleton by linear actuator. The main focus is to use an actuator with a conversion from rotary to linear output with the help of leadscrew. Dollar and Hugh [1] created a lower-limb exoskeleton to make running easier. A motorized mechanism in the device's knee brace actively inserts and removes a spring that runs parallel to the knee joint. This exoskeleton has the benefit of requiring less energy from the quadriceps to perform this function but has the disadvantage of depending on an external power source. A tethered knee exoskeleton with a light-weight frame and four points of contact with the leg was created by Ann et al. [25]. The exoskeletons were designed based on cable tension and Pulley. They wanted to research robotic support techniques to improve gait rehabilitation and improve human athletic ability using this knee exoskeleton, although it has drawbacks due to its big size and design. In order to operate as a rehabilitation tool or a single joint add-on exoskeleton device for power augmentation, Saccares et al. [26] developed an iT-Knee, a modular knee exoskeleton that will use a torque transmission interface to transmit pure assistive torque to the knee articulation. Zhao and Song [27] designed an exoskeleton with the help of pneumatic muscle actuators (PMAs). To provide accurate trajectory tracking, a proxy-based sliding mode control is used in order to achieve greater performance for the proposed PMA-based exoskeleton when compared to traditional control techniques.

Ramanpreet et al. [28] developed a four-bar exoskeleton design for lower limb exoskeleton (LLE) to support in walking, A mechanism is developed that can be used in the rehabilitation of knee. Singh et al. [29] developed a novel approach for the synthesis of four-bar linkage by using a realistic gait trajectory. Using a two-stage optimization process, the error between the generated and desired hip trajectories is reduced. The hybrid teaching-learning-particle-swarm-optimization is used to address the optimization challenge.

Studies in the literature indicate that the stainless-steel pipes will be the main component of the frame and polyethylene terephthalate glycol, commonly known as PETG, for the motor mountings. They settled with stainless steel 304. Ranaweera et al. [30] used acrylic glass for passively powered knee exoskeleton. Najam et al. [31] reported that the aluminum alloy AA7068 is an appropriate material to manufacture the exoskeleton knee. However, the stated that Al7068 it is not available. The titanium alloys were the second choice but they were too expensive. Then they suggested Mg alloys. The advantage of Mg alloy compared to metal alloy is that it is lightest of all metal alloys and has density and Young's modulus nearly same as that of bone. After that they tried to test a different composite that can be used for the exoskeleton frame. The carbon fiber is the most appropriate composite. Finally, they settled with Al7075 as the appropriate option. The most suitable material according to their results is Al7075 and carbon fiber depending on the model they have achieved of the mechanical properties. The results were computed for a person weighing 91 kg. Bjoner and Hole [32] compared Al6061-T6 and Al7075-T6. They stated that Al6061-T6 is more ductile but has less strength than Al7075-T6. de las Heras [33] had used an alloy that can recover to its original shape after it was exposed to a heat element, the alloy is called shape memory alloy (SMA). Most common SMA is nitinol, a combination of nickel and titanium. The material is austenite at high temperature, and martensite at lower temperatures. They have used very small SMA wires and passing DC electric current through them which will increase the wire temperature applying the Joule Effect. Bair [34] suggested four materials for the knee exoskeleton: aluminum 6061-T6, steel low carbon, steel 4140, and titanium grade 5. They chose aluminum 6061-T6 because of its strength, lightweight, and affordable price to manage the mechanical demands. Chen et al. [35] have adjusted the height of the exoskeleton in a range between 1.55 and 1.85 m. They made it from aluminum alloy (7075-T651) in order to achieve lightweight and high stiffness. To develop a LLE, Nimavat et al. [36] selected aluminum alloy 356 and standard carbon fiber. They found that aluminum can carry an yield Strength of about 166 MPa with Young's Modulus of 72 GPa and the standard carbon fiber can carry and yield strength of 1,080 MPa and Young's modulus of 70 GPa.

The main goal of this study is to propose a new gait-inspired method based on a genetic algorithm (GA) for synthesizing a four-bar mechanism for exoskeletons. The optimal design for a LLE will be depicted as a solid model and simulated for a realistic gait cycle.

2 Modeling of an exoskeleton with four bars and natural trajectory

A healthy lower limb must ensure the swing and stance phases of the gait cycle during human leg motion. During the swing phase, one limb begins the motion in the forward direction while another limb designates the stance phase by pivoting to the ground. A complete gait cycle is achieved when each limb passes through swing and stance phases as presented in Figure 1.

The LLE is represented in Figure 1. The foot is the target of one connection, while the hip is the target of the other. The links are extended in length to capture the foot and hip joint trajectories when walking. The expanded connections' lengths are constrained so that the center of the four-bar linkage maintains alignment with the position of a normal human knee joint. For a healthy person, the boundary limitations for the extended links, which are employed for the thigh and shank, can be evaluated.

The synthesis procedure of LLE is typically a call for a reference frame, XOY, on the LLE that is anchored to the walking surface, as shown in Figure 1. For the whole gait cycle, the height of the hip from the flat surface, h, is assumed to be a constant number, and the foot is assumed to be a point. Point B represents the hip. The exoskeleton is characterized by the links FE, ED, FH, and DH, with CB and GP being extensions of the FE, ED, FH, and DH. ED and FH are linked together. FH, FE, ED, and DH have different link lengths r_1; r_2; r_3, and r_4, respectively. θ_{1sw}; θ_{2sw}; θ_{3sw}, and θ_{4sw} are the orientations of the r_1; r_2; r_3, and r_4 in swing phase, respectively. The lengths of the extended linkages are as follows: GP and CB are categorized as l_3 and l_4, respectively, and are 90° to r_1 and r_3 at the midpoint of their linkages. As illustrated in Figure 1, the lengths l_1 and l_2 specified by OA and AB are articulated at point A through the revolute joint. The HLL linkages OA and AB are orientated at first and second angles with regard to the axis-X, respectively.
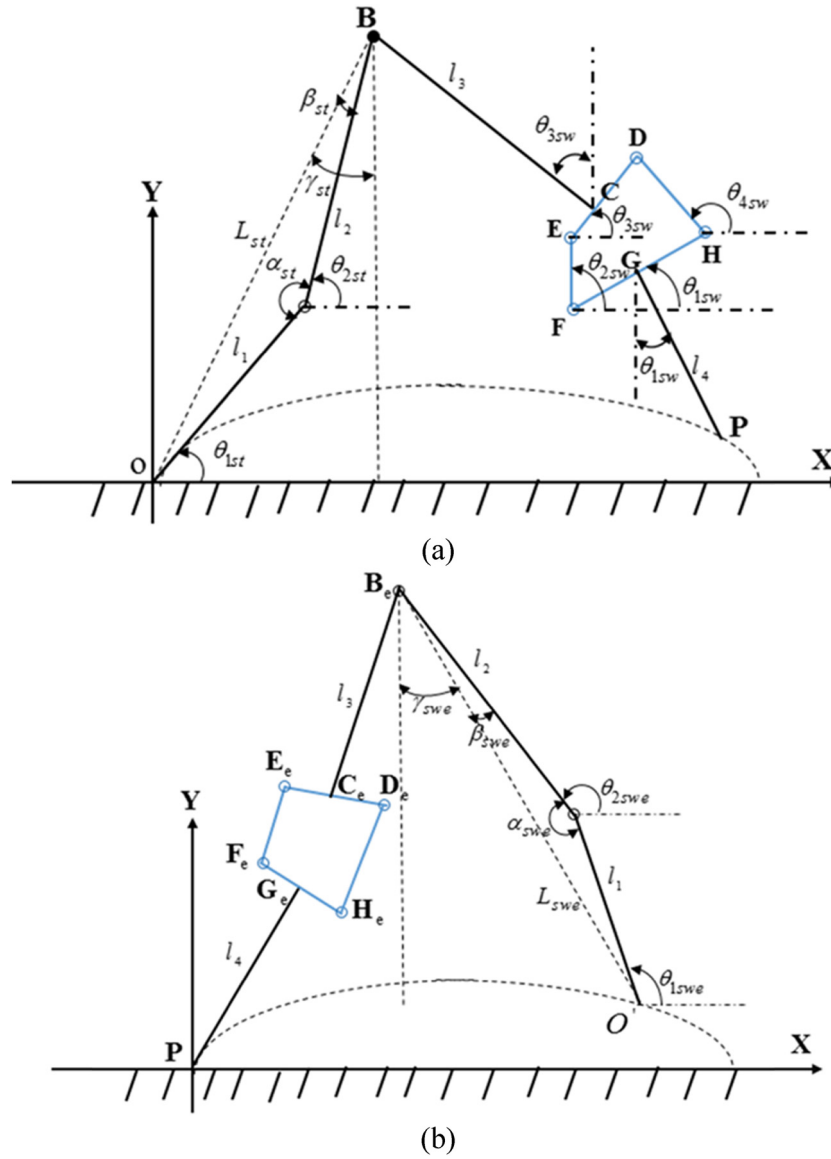
Figure 1: LLE during a gait cycle; (a) swing phase and (b) stance.

The limb in stance phase is denoted by the subscript st. The other parameters needed for joint profile construction are: L_{st}, the distance between origin O and point B; γ_{st}, the angle between the Y-axis traveling through B and virtual link OB; β_{st}, the angle between links AB and OB; and θ_{2sty}, the angle between the Y-axis passing through B and link AB.

The coordinates of the hip, B_x, and B_y are given as input. Thus, coordinates of C, E, F, and G are given as follows:

$$C_x = B_x + l_3\cos\left(\frac{3\pi}{2} + \theta_{3sw}\right), \tag{1}$$

$$C_y = B_y + l_3\sin\left(\frac{3\pi}{2} + \theta_{3sw}\right), \tag{2}$$

$$E_x = C_x + \frac{r_3}{2}\cos(\pi + \theta_{3sw}), \tag{3}$$

$$E_y = C_y + \frac{r_3}{2}\sin(\pi + \theta_{3sw}), \tag{4}$$

$$F_x = E_x + r_2\cos(\pi + \theta_{2sw}), \tag{5}$$

$$F_y = E_y + r_2\sin(\pi + \theta_{2sw}), \tag{6}$$

$$G_x = F_x + \frac{r_1}{2}\cos(\theta_{1sw}), \tag{7}$$

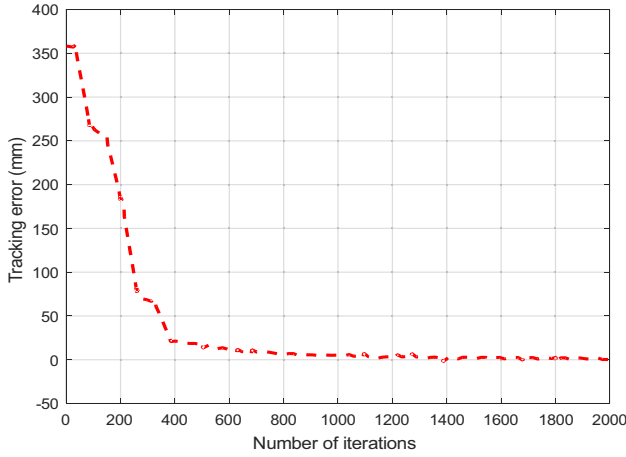$$G_y = F_y + \frac{r_1}{2}\sin(\theta_{1sw}). \tag{8}$$

Figure 2: Number of iterations.

- Foot point P of the LLE's swing phase trajectories are as follows:

$$P_x = G_x + l_4\cos\left(\frac{3\pi}{2} + \theta_{1sw}\right), \qquad (9)$$

$$P_y = G_y + l_4\sin\left(\frac{3\pi}{2} + \theta_{1sw}\right). \qquad (10)$$

- The LLE's stance phase trajectories are calculated as follows:

$$G_{ex} = P_x + l_4\cos\left(\frac{\pi}{2} + \theta_{1ste}\right), \qquad (11)$$

$$G_{ey} = P_y + l_4\sin\left(\frac{\pi}{2} + \theta_{1ste}\right), \qquad (12)$$

$$F_{ex} = G_{ex} + \frac{r_1}{2}\cos(\pi + \theta_{1ste}), \qquad (13)$$

$$F_{ey} = G_{ey} + \frac{r_1}{2}\sin(\pi + \theta_{1ste}), \qquad (14)$$

$$E_{ex} = F_{ex} + r_2\cos(\pi + \theta_{2ste}), \qquad (15)$$

Table 1: Design variables at swing and stance phase

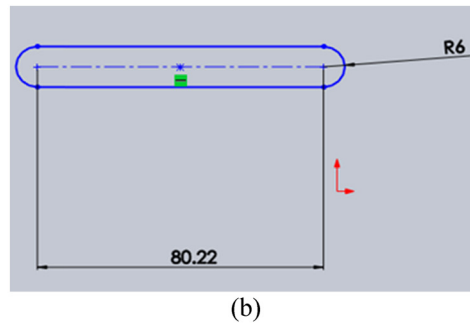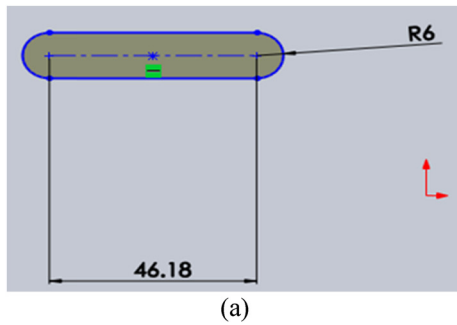| Design variables	Swing phase	Design variables	Stance phase
r_1	82.53	θ_{1ste}^1	2.606
r_2	46.18	θ_{1ste}^2	2.822
r_3	72.97	θ_{1ste}^3	2.756
r_4	80.22	θ_{1ste}^4	2.986
l_3'	285.16	θ_{1ste}^5	2.944
l_4'	265.36	θ_{1ste}^6	2.855
θ_{1sw}^1	1.12	θ_{1ste}^7	2.616
θ_{1sw}^2	1.81	θ_{1ste}^8	2.508
θ_{1sw}^3	0.35	θ_{1ste}^9	2.344
θ_{1sw}^4	2.78	θ_{1ste}^{10}	2.033
θ_{1sw}^5	0.06	θ_{2ste}^1	6.288
θ_{1sw}^6	3.18	θ_{2ste}^2	6.198
θ_{1sw}^7	0.538	θ_{2ste}^3	6.055
θ_{1sw}^8	2.867	θ_{2ste}^4	5.908
θ_{1sw}^9	1.505	θ_{2ste}^5	5.892
θ_{1sw}^{10}	1.922	θ_{2ste}^6	5.811
θ_{2sw}^1	5.699	θ_{2ste}^7	5.765
θ_{2sw}^2	6.024	θ_{2ste}^8	5.722
θ_{2sw}^3	5.812	θ_{2ste}^9	5.701
θ_{2sw}^4	5.503	θ_{2ste}^{10}	5.678
θ_{2sw}^5	5.887	TE = 0.0236 mm	
θ_{2sw}^6	5.814		
θ_{2sw}^7	6.111		
θ_{2sw}^8	6.098		
θ_{2sw}^9	3.277		
θ_{2sw}^{10}	0.056		

Figure 3: Sketch of links (a) r_2 and (b) r_4.

Table 2: Comparison between PSO, HTLPSO, and GA

	Optimization method	Minimum TE (mm)	Number of iterations
Ramanpreet et al., 2017 [28]	Particle-swarm-optimization	0.052	5,600
Singh et al., 2019 [29]	Hybrid teaching-learning-particle-swarm-optimization	0.486	3,700
This study	GA	0.0236	2,000
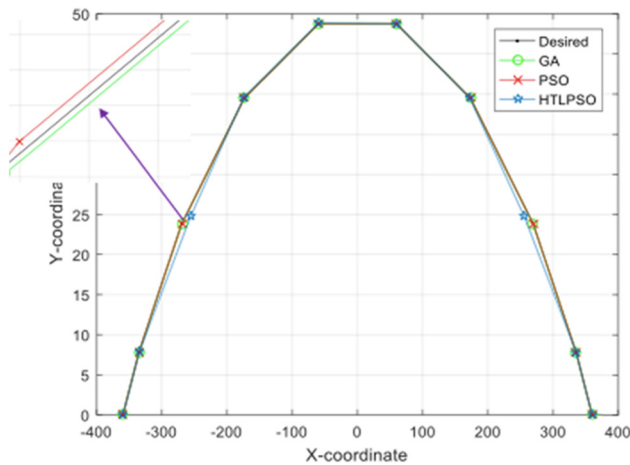
Figure 4: Comparison of swing phase foot trajectory.
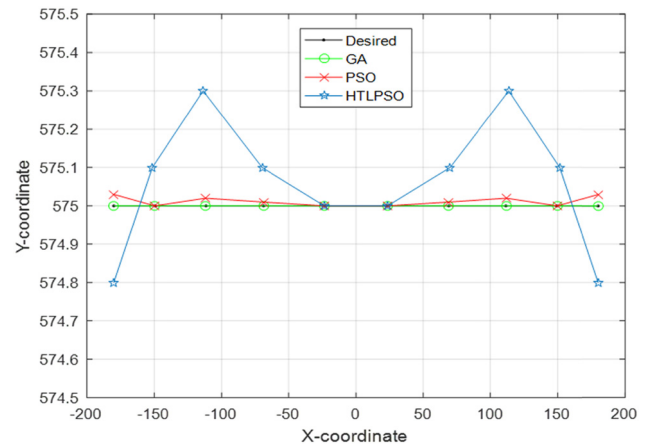
Figure 5: Hip trajectory comparisons during the stance phase.

$$E_{ey} = F_{ey} + r_2\sin(\pi + \theta_{2\text{ste}}), \quad (16)$$

$$C_{ex} = E_{ex} + \frac{r_3}{2}\cos(\theta_{3\text{ste}}), \quad (17)$$

$$C_{ey} = E_{ey} + \frac{r_3}{2}\sin(\theta_{3\text{ste}}). \quad (18)$$

- Trajectories of the hip point B of LLE in stance phase are as follows:

$$B_{ex} = C_{ex} + l_3\cos\left(\frac{\pi}{2} + \theta_{3\text{ste}}\right), \quad (19)$$

$$B_{ey} = C_{ey} + l_3\sin\left(\frac{\pi}{2} + \theta_{3\text{ste}}\right), \quad (20)$$

- Objective function of the optimization problem

$$\text{minimize TE} = \sum_{k=1}^{n}\sqrt{(P_x^k - P_{xd}^k)^2 + (P_y^k - P_{yd}^k)^2} + \sum_{k=1}^{N}\sqrt{(B_{ex}^k - B_{exd}^k)^2 + (B_{ey}^k - B_{eyd}^k)^2}. \quad (21)$$

(i) Grashof constraint

$$g_1(X) = r_1 + r_2 - r_3 - r_4 < 0 \quad \text{if} \quad (r_2 < r_3 < r_4 < r_1). \quad (22)$$

(ii) Constant height for gait cycle

$$g_2(X) = l_3 + l_4 - h < 0. \quad (23)$$

(iii) Range of variables

$$L_i \le x_i \le U_i,$$

$$\theta_{1m}^k \in [0.\ 2\pi], \quad \theta_{2m}^k \in [0.\ 2\pi], \quad r_1 \in [20.\ 90],$$
$$r_2 \in [40.\ 170], \quad r_3 \in [20.\ 90],$$
$$r_4 \in [40.\ 170], \quad l_3 \in [180.\ 320], \quad l_4 \in [180.\ 320].$$

3 Procedure of optimization

With the introduction of the digital computer and artificial intelligence method in the early 50s, interest in the optimization process has taken a giant leap. Optimization methods have progressed steadily in recent years and significant progress has been made. Digital computers have become quicker, more flexible, and more powerful at the same time. As a result, complex optimization problems that just a few years ago were considered to be intractable can now be solved [37]. The choice of the optimization method depends essentially on the nature, number of the design parameters and performance to be optimized. Thus, there are two families of optimization methods. Deterministic methods are those that are
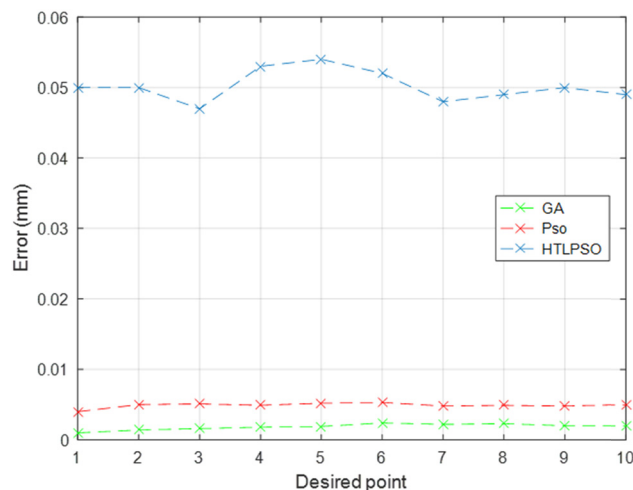
Figure 6: Evolution of error as function of desired points.

Figure 8: Prototype mechanism assembled.

characterized by a methodical and systematic choice of design parameters and their research fields [38]. Stochastic methods are characterized by a random choice of design parameters in their fields of research [39]. There are several stochastic optimization methods. The most famous is the GA. The evolutionary algorithm, which includes the GA, is founded on the principle of natural selection. Johen Holland implemented the fundamental concepts of GA at the University of Michigan in 1970 [40]. GA is a stochastic method that does not require mathematical formulation. According to conventional programming techniques, it has emerged as important in solving large complex problems that require a long time, where the solution is either optimal or close to optimal, over a suitable time [41].

The proposed design method is applied to synthesize a four-bar linkage exoskeleton. The healthy participant's preferred foot and hip trajectories are derived from a gait database [30]. Material selection is a very important stage to avoid failures and surface roughness and achieve stability, which leads to better life period and good user experience. The material should be light to reduce burden on the body. The cost limitation forces to select a material that is affordable to the patient, which will limit the usage of the material proposed in the previous studies. The prototype material is polylactic acid (PLA) which was chosen for manufacturing the prototype for testing purposes, to prevent any undesired final output. This polymer can be worn to show the mechanism behavior while walking.

Fused filament fabrication (FFF) is one of the recent ways to shape polymer specially PEEK in FFF 3D printer.
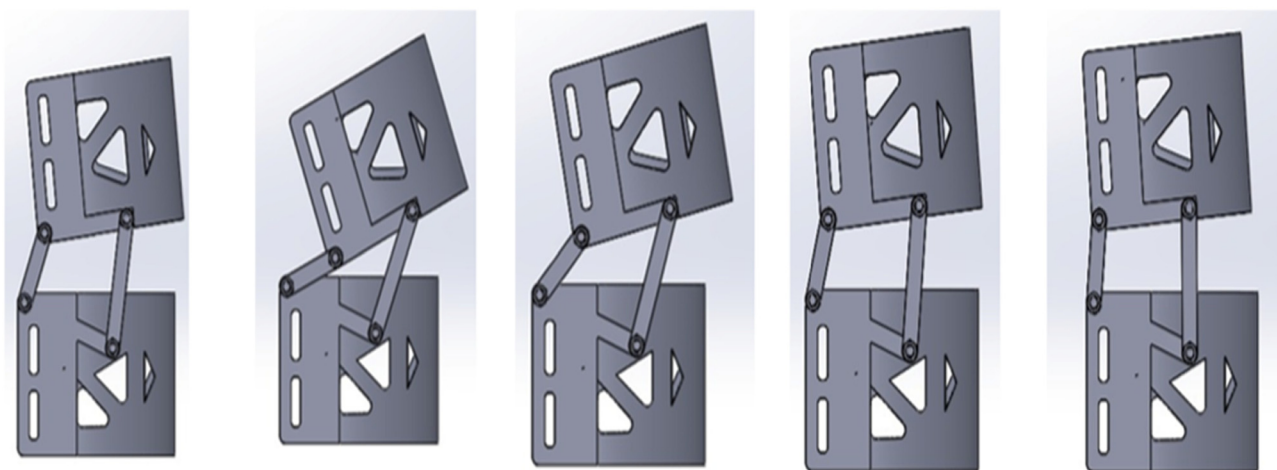
Figure 7: Model and simulation of the proposed LLE design in SolidWorks.
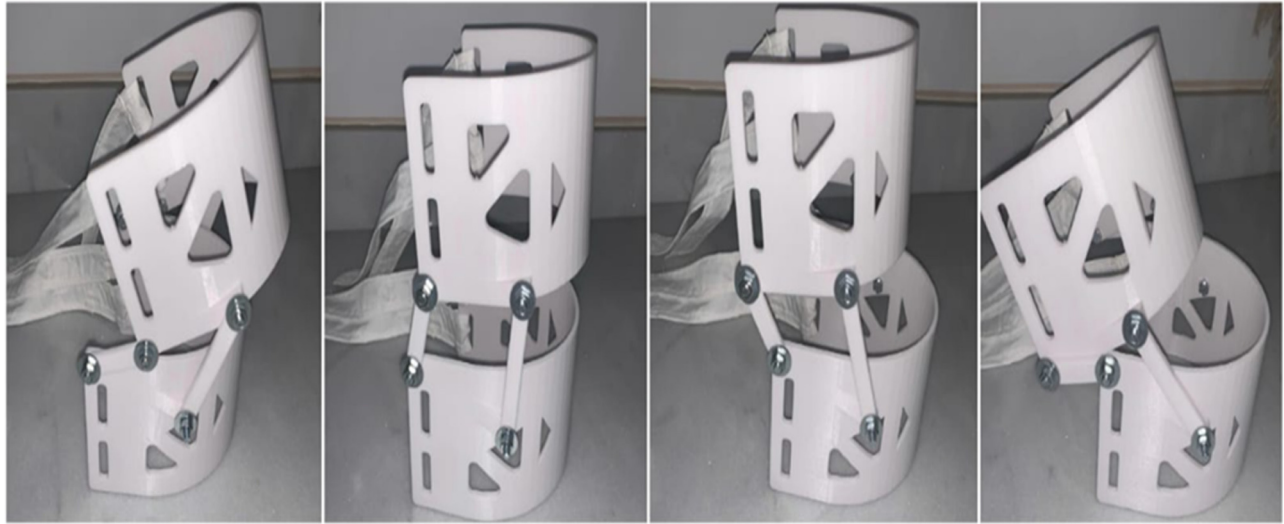
Figure 9: Swing phase and the stance phase.

FFF uses a continuous filament of polymer material fed from a large coil into heat printer extruder and then molten material is forced out of the nozzle and deposited on a growing work piece. FFF is dependent on material heat transfer properties and rheology. FFF has many advantages such as low start-up time, low maintenance, quick to repair, and easy to clean [20].

4 Results

The first of three parts in this section presents the numerical outcomes of our approach. The second section contrasts our findings with those of other studies. The manufacturing results are discussed in the final section. Figure 2 presents how many times the GA is to be run to find the optimum solution, which was found just after 2,000 iterations when the tracking error was at minimum. In addition, Table 1 shows the optimal design variables for both swing and stance phases coupled with the minimum tracking error.

The optimized linkage dimensions are $r_1 = 82.53$, $r_2 = 46.18$, $r_3 = 72.97$, $r_4 = 80.22$, $l_3' = 285.16$, and $l_4' = 265.36$. The minimum tracking error = 0.0236. Figure 3 shows the design sketch of both r_2 and r_4, respectively, with their dimensions, both of them have a thickness = 4 mm.

To evaluate the GA efficacy, the same optimization problem is solved in literature by the particle-swarm-optimization

Figure 10: Testing knee exoskeleton prototype.

algorithm and the hybrid teaching-learning-particle-swarm-optimization method developed by Ramanpreet et al. [28] and Singh et al. [29], respectively. The evolution of TE as function of the number of iterations, for the best four-bar exoskeleton design, is presented in Table 2. One can note that the lower value of TE is given by GA, compared with GA and MOPSO and with fewer iteration value. In fact, GA reached an optimum value of 0.0236 mm in 2,000 iterations, PSO offered 0.052 mm in 5,600 iterations and HTLPSO provided 0.486 mm in 3,700 iterations. Thus, GA is capable to improve the TE results of PSO and HTLPSO by about 54 and 96%, respectively.

Figures 4 and 5 display the plots of the required and generated foot- and hip-trajectories achieved using GA, HTLPSO, and PSO. From Figures 4 and 5, it is clear that, in swing phase, the GA is the closest to the desired trajectory rather than HTLPSO and PSO. Moreover, the GA gives better results, and also, in the stance phase, the GA passes accurately through all desired points, while HTLPSO and PSO do not accurately pass through the desired points, which gives a confirmation that the GA results are better than the HTLPSO and PSO in tracking the desired points.

Figure 6 displays the sum of error in swing and stance phases and compares between GA, PSO, and HTLPSO. As shown in Figure 6, the GA is the closest to the desired output rather than HTLPSO and PSO, which means the GA had the smallest error value in both the swing and stance phases.

The designed four-bar linkage has been modeled and simulated by using SolidWorks Software. Figure 7 shows five postures of designed linkages. After designing, the prototype was manufactured using a 3D-printer All parts were printed with good accuracy that can confidently be tested as worn mechanism. Figure 8 represents the assembly of the mechanism. Figure 9 illustrates the swing and stance phases from the right to the left.

Figure 10 depicts how the prototype was worn on the leg. In the swing and stance phases, it is flexible. If this linkage is fixed to a user, their lower limb can deliver the necessary trajectories for one gait cycle. Therefore, any application that requires walking can use the specified linkage.

5 Conclusion

The four-bar linkage synthesis for the LLE during walking was suggested in this research work. In an absolute frame that is fixed to the ground, the foot and hip trajectories

are determined. In the form of a multistage optimization algorithm, the synthesis problem is presented. The goal is to minimize, simultaneously, the Euclidean distance between the desired and generated limb trajectories in swing and stance phases. The GA is employed to find a workable solution, and the outcomes are compared to those of the well-known literature methods. It is discovered that GA converges to an optimal value of TE less than PSO results and HTLPSO results by 54% and 96%, respectively. As a result, for this problem, GA is a computationally more effective method than PSO and HTLPSO. Simulating the synthesized linkage in SolidWorks is also done in order to test the lower limb's gait for an entire gait cycle, and a stick diagram of the lower limb while walking is also shown. The poses of linkage during flexion are also shown using a realistic prototype. Thus, the portable leg exoskeleton or any other rehabilitation device can be utilized with the designed four-bar linkage, which can track the desired trajectory. This approach is workable to create the four-bar connection essential for walking, for example, in humanoid robots, robotic arms, orthoses, etc. A minor adjustment to the suggested methodology can be used to create flexible and unique mechanisms. Moreover, by using controller equipment on the passive mechanism created to support the damaged knee joint, the work can be extended.

Conflict of interest: The authors declare no conflict of interest.

References

[1] Dollar AM, Hugh H. Design of a quasi-passive knee exoskeleton to assist running. 2008 IEEE/RSJ International Conference on Intelligent Robots and Systems. IEEE, 2008 Rehabilitation. International Journal of Computer Applications 62, no. 1310.1109/IROS.2008.4651202; 2018.

[2] Bogue R. Robotic exoskeletons: a review of recent progress. Ind Robot An Int J. 2015;42(1):5–10. doi: 10.1108/IR-08-2014-0379.

[3] Cao J, Vijay V. Design of a lower extremity exoskeleton to improve gait in elderly patients with knee osteoarthritis by reducing knee joint loading. Denton, Texas, USA: University of North Texas; 2016. https://hdl.handle.net/20.500.12503/26697.

[4] Diaz I, Jorge JG, Emilio S. Lower-limb robotic rehabilitation: Literature review and challenges. J Robot. 2011;2011:1–12. doi: 10.1155/2011/759764.

[5] Dam M, Tonin P, Casson S, Ermani M, Pizzolato G, Iaia V, et al. The effects of long-term rehabilitation therapy on poststroke hemiplegic patients. Stroke. 1993;24(8):1186–91. doi: 10.1161/01.str.24.8.1186.

[6] Smith DS, Goldenberg E, Ashburn AE, Kinsella G, Sheikh K, Brennan PJ, et al. Remedial therapy after stroke: a randomised controlled trial. Br Med J. 1981;282(6263):517–20. doi: 10.1136/bmj.282.6263.517.

[7] Krebs HI, Volpe BT, Aisen ML, Hogan N. Increasing productivity and quality of care: Robot-aided neuro-rehabilitation. J Rehabil Res Dev. 2000;37(6):639.

[8] Beyl P, Michaël Van D, Ronald Van H, Rino V, Bram V, Dirk L. An exoskeleton for gait rehabilitation: prototype design and control principle. IEEE International Conference on Robotics and Automation 2008. ICRA 2008. IEEE; 2008. p. 2037–42. doi: 10.1109/ROBOT.2008.4543506.

[9] Norouzi-Gheidari N, Archambault PS, Fung J. Effects of robot-assisted therapy on stroke rehabilitation in upper limbs: systematic review and meta-analysis of the literature. J Rehabil Res Dev. 2012;49(4):479. doi: 10.1682/jrrd.2010.10.0210.

[10] Trumble TN. The use of nutraceuticals for osteoarthritis in horses. Vet Clin Equine Pract. 2005;21(3):575–97. doi: 10.1016/j.cveq.2005.08.004.

[11] Longstaff LM, Sloan K, Stamp N, Scaddan M, Beaver R. Good alignment after total knee arthro-plasty leads to faster rehabilitation and better function. J arthroplasty. 2009;24(4): 570–78. doi: 10.1016/j.arth.2008.03.002.

[12] Toutoungi DE, Lu TW, Leardini A, Catani F, O'connor JJ. Cruciate ligament forces in the human knee during rehabilitation exercises. Clin Biomech. 2000;153:176–87. doi: 10.1016/ s0268-0033(99)00063-7.

[13] Rupal BS, Singla A, Virk GS. Lower limb exoskeletons: a brief review. In Conference on Mechanical Engineering and Technology (COMET-2016). Varanasi, India: IIT (BHU); 2016. p. 130–40. doi: 10.17586/2226-1494-2017-17-6-1153-1158.

[14] Fasoli SE. Rehabilitation technologies to promote upper limb recovery after stroke, in stroke rehabilitation. Stroke Rehabilitation. Amsterdam, Netherlands: Elsevier; 2016. p. 486–5. doi: 10. 10.1016/B978-0-323-17281-3.00022-8.

[15] Khorshidi M, Soheilypour M, Peyro M, Atai A, Shariat Panahi M. Optimal design of four-bar mechanisms using a hybrid multi-objective GA with adaptive local search. Mech Mach Theory. 2011;46(10):1453–65. doi: 10.1016/j. mechmachtheory.2011.05.006.

[16] Tucker MR, Olivier J, Pagel A, Bleuler H, Bouri M, Lambercy O, et al. Control strategies for active lower extremity prosthetics and orthotics: a review. J Neuroeng Rehabil. 2015;12(1):1.

[17] Vukobratovic M, Hristic D, Stojilj kovic Z. Development of active anthropomorphic exoskeletons. Med Biol Eng. 1974;12(1):66–80.

[18] Kim JH, Shim M, Ahn DH, Son BJ, Kim SY, Kim DY, et al. Design of a Knee Exoskeleton Using Foot Pressure and Knee Torque Sensors. Int J Adv Robotic Syst. 2015;12(8). doi: 10.5772/6078.

[19] Probsting E, Kannenberg A, Zacharias B. Safety and walking ability of KAFO users with the C-Brace Orthotronic Mobility System, a new microprocessor stance and swing control orthosis. Prosthet Orthot Int. 2017;41(1):65–77.

[20] Lu Z, Huo J, Wang Y, Xin T, Xie Z. Design and simulation analysis of a lower limbs exoskeleton powered by hydraulic drive.

2017 2nd International Conference on Advanced Robotics and Mechatronics (ICARM); 2017. p. 173–7. doi: 10.1109/ICARM. 2017.8273155.

[21] Niu Y, Song Z, Dai J. Kinematic analysis and optimization of a planar parallel compliant mechanism for self-alignment knee exoskeleton. Mech Sci. 2018;9(2):405–16. https://ms. copernicus.org/articles/9/405/2018/ms-9-405-2018.pdf.

[22] Kittisares S, Nabae H, Endo G, Suzumori K, Sakurai R. Design of knee support device based on four-bar linkage and hydraulic artificial muscle. Robomech J. 2020;7(1):1–10.

[23] Gao M, Wang Z, Li S, Li J, Pang Z, Liu S, et al. Design and optimization of exoskeleton structure of lower limb knee joint based on cross four-bar linkage. AIP Adv. 2021;11(6):1–12. doi: 10.1063/5.0053899.

[24] Putranto ID, Budiarto E, Kidarsa LA. Mechanical Design of Knee and Ankle Exoskeleton to Help Patients with Lower Limb Disabilities. Proceedings of the 11th National Congress and the 18th Annual Scientific Meeting of Indone-sian Physical Medicine and Rehabilitation Association; 2019. doi: 10.5220/ 0009061600160027.

[25] Witte KA, Fatschel AM, Collins SH. Design of a lightweight, tethered, torque-controlled knee exoskeleton. 2017 International Conference on Rehabilitation Robotics (ICORR). New Jersey, United States: IEEE; 2017. doi: 10.1109/ICORR. 2017.8009484.

[26] Saccares L, Sarakoglou I, Tsagarakis NG. iT-Knee: An exoskeleton with ideal torque transmission interface for ergonomic power augmentation. 2016 IEEE/RSJ International Conference on Intelligent Robots and Systems (IROS). New Jersey, United States: IEEE; 2016.

[27] Zhao W, Song A. Active Motion Control of a Knee Exoskeleton Driven by Antagonistic Pneumatic Muscle Actuators. Actuators. 2020;9(4):134. doi: 10.3390/act9040134.

[28] Ramanpreet S, Himanshu CH, Amit Kumar S. A novel gait inspired four-bar lower limb exoskeleton to guide the walking movement. J Mech Med Biol. 2019;19(4):1–24. doi: 10.1142/ S0219519419500209018.

[29] Singh R, Chaudhary H, Singh AK. A novel gait-based synthesis procedure for the design of 4-bar exoskeleton with natural trajectories. J Orthop Transl. 2017 Nov 20;12:6–15. doi: 10.1016/j.jot.2017.09.001PMID: 29662774; PMCID: PMC5866500.

[30] Ranaweera RKPS, Gopura RARC, Jayawardena TSS, Mann GKI. Development of A passively powered knee exoskeleton for squat lifting. J Robot Netw Artif Life. 2018;5(1):45.

[31] Najam H, Bal B, Unal R. Material selection for knee exoskeleton frame. In The Internationon Conference on Materi-als Science, Mechanical and Automotive Engineerings and Technology; 2018.

[32] Bjoner J, Hole R. Development of a passive lower body exoskeleton with novel compliant joints for walking assistance; 2020. https://projekter.aau.dk/projekter/files/334369853/ DMS4_Group23D_MasterThesis.pdf.

[33] de las Heras DG. Design of a knee exoskeleton actuated with artificial muscles of SMA. Core.ac.uk; 2018. https://core.ac. uk/download/pdf/288501543.pdf.

[34] Bair MO. The design and testing of a powered exoskeleton to reduce the metabolic cost of walking in individuals with cerebral palsy. Core.ac.uk; 2018. https://core.ac.uk/download/ pdf/162614001.pdf.

[35] Chen S, Wang Y, Li S, Wang G, Huang Y, Mao X. Lower limb rehabilitation robot. ASME/IFToMM International conference on reconfigurable mechanisms and robots. London: IEEE; 2009. p. 439–43.

[36] Nimavat D, Parasara H, Hansalia H, Parmar D. Innovative Design of Mechanical Leg Exoskeleton as an External Knee Joint Apparatus, and Human Leg Augmentation or leg Assistive Device. IIIE's International Conference on Smart Strategies for Digital World At. India: IIIE- Nagpur; 2016.

[37] Vukobratovic M, Hristic D, Stojiljkovic Z. Development of active anthropomorphic exoskeletons. Med Biol Eng. 1974;12(1):66–80.

[38] Strausser KA, Kazerooni H. The development and testing of a human machine interface for a mobile medical exoskeleton.

2011 IEEE/RSJ International Conference on Intelligent Robots and Systems; 2011. p. 4911–6.

[39] Dollar AM, Herr H. Design of a quasi-passive knee exoskeleton to assist running. 2008 IEEE/RSJ Internation-al Conference on Intelligent Robots and Systems. IEEE; 2008.

[40] Shukla A, Pandey H, Mehrotra D. Comparative Review of Selection Techniques in Genetic Algorithm. 2015 In-ternational Conference on Futuristic Trends on Computational Analysis and Knowledge Management (ABLAZE); 2015.

[41] Mishra P, Das D, Ukamanal M, Routara B, Sahoo A. Multi-response optimization of process parameters using Taguchi method and grey relational analysis during turning AA 7075/ SiC composite in dry and spray cooling environments. Int J Ind Eng. 2015;6:445–56.